Drug glucuronidation assays on human liver microsomes immobilized on microfluidic flow-through reactors

Kiiski, Iiro

2021-03-01

Kiiski , I , Ollikainen , E , Artes , S , Järvinen , P , Jokinen , V & Sikanen , T 2021 , ' Drug glucuronidation assays on human liver microsomes immobilized on microfluidic flow-through reactors ' , European Journal of Pharmaceutical Sciences , vol. 158 , 105677 . https://doi.org/10.1016/j.ejps.2020.105

http://hdl.handle.net/10138/325598
https://doi.org/10.1016/j.ejps.2020.105677

European Journal of Pharmaceutical Sciences 158 (2021) 105677

Contents lists available at ScienceDirect

European Journal of Pharmaceutical Sciences

journal homepage: www.elsevier.com/locate/ejps

Drug glucuronidation assays on human liver microsomes immobilized on microfluidic flow-through reactors

Iiro Kiiski [a], Elisa Ollikainen [a], Sanna Artes [a], Päivi Järvinen [a], Ville Jokinen [b], Tiina Sikanen [a,*]

[a] Drug Research Program, Division of Pharmaceutical Chemistry and Technology, Faculty of Pharmacy, University of Helsinki, P.O. Box 56 (Viikinkaari 5E), FI-00014 University of Helsinki, Finland
[b] Department of Materials Science and Engineering, School of Chemical Engineering, Aalto University, FI-02150 Espoo, Finland

ARTICLE INFO

Keywords:
Drug metabolism
Glucuronidation
Microreactors
Enzyme immobilization
Microfluidics
Microfabrication

ABSTRACT

UDP-glucuronosyltransferases (UGTs), located in the endoplasmic reticulum of liver cells, are an important family of enzymes, responsible for the biotransformation of several endogenous and exogenous chemicals, including therapeutic drugs. However, the phenomenon of 'latency', i.e., full UGT activity revealed by disruption of the microsomal membrane, poses substantial challenges for predicting drug clearance based on *in vitro* glucuronidation assays. This work introduces a microfluidic reactor design comprising immobilized human liver microsomes to facilitate the study of UGT-mediated drug clearance under flow-through conditions. The performance of the microreactor is characterized using glucuronidation of 8-hydroxyquinoline (via multiple UGTs) and zidovudine (via UGT2B7) as the model reactions. With the help of alamethicin and albumin effects, we show that conducting UGT metabolism assays under flow conditions facilitates in-depth mechanistic studies, which may also shed light on UGT latency.

1. Introduction

Enzymatic biotransformations via cytochrome P450 (CYP) and UDP-glucuronosyltransferase (UGT) systems are the major elimination pathways for most xenobiotic compounds, including therapeutic drugs (Williams et al., 2004). The CYP enzyme family catalyzes oxidoreductive reactions that introduce new functional moieties into the drug molecule, whereas the UGTs catalyze the addition of a glucuronic acid moiety into a drug, resulting in a water-soluble metabolite that is easily excreted from the body through bile or urine. While disturbances in CYP function are known to result in a myriad of clinically relevant drug-drug interactions (DDI), glucuronide metabolites of therapeutic drugs are generally regarded as being inert and non-toxic. However, some drugs can also form unstable acyl glucuronides that possess cytotoxic properties (Regan et al., 2010) or act as irreversible inhibitors of CYPs, leading to interactions of clinical consequence associated particularly with CYP2C8 (Backman et al., 2009; Tornio et al., 2014). Excessive glucuronidation may also result in complete loss of drug efficacy. For example, raloxifene, a widely used drug in the treatment of osteoporosis, has a poor oral bioavailability (2%) due to its extensive presystemic glucuronidation (Hochner-Celnikier, 1999). On the other hand, morphine 6-glucuronide is an even more potent analgesic than the parent molecule itself (Klimas and Mikus, 2014). Consequently, preclinical screening for UGT-mediated drug clearance (enzyme kinetics) and the interlinked DDIs is an essential part of the regulatory guidance for the pharmaceutical industry (EMA, 2012; FDA, 2020). On one hand, several *in silico* methods have been introduced to date in the effort to predict the metabolic fate of drugs. The construction of reliable computational models remains a challenge, however, and necessitates the use of experimental validation datasets (Kazmi et al., 2019). For this purpose, both *in vitro* human models and *in vivo* animal models are used. The species-specific differences, e.g., unique or disproportionate metabolites produced in laboratory animals, possess yet another challenge to preclinical prediction of the metabolic fate of new drug candidates (Issa et al., 2017), leaving the *in vitro* assays on human-derived enzyme sources (i.e., cells and subcellular microsomal fractions) as the most feasible model for prediction of human drug metabolism *in vitro*.

A significant challenge with human UGT assays *in vitro* is their limited capability to predict the intrinsic drug clearance (CL_{int}) *in vivo*. As the UGT enzymes are membrane proteins embedded in the endoplasmic reticulum (ER) of liver cells, with the active site facing the luminal side (Tukey and Strassburg, 2000), the ER membrane forms a

* Corresponding author.
E-mail addresses: iiro.kiiski@helsinki.fi (I. Kiiski), elisa.ollikainen@helsinki.fi (E. Ollikainen), sanna.artes@helsinki.fi (S. Artes), paivi.jarvinen@helsinki.fi (P. Järvinen), ville.p.jokinen@aalto.fi (V. Jokinen), tiina.sikanen@helsinki.fi (T. Sikanen).

https://doi.org/10.1016/j.ejps.2020.105677
Received 24 July 2020; Received in revised form 6 November 2020; Accepted 7 December 2020
Available online 10 December 2020

physical barrier to the drug substrates. As a result, significant underestimation of drug glucuronidation is often associated with *in vitro* assays performed with hepatocytes or isolated microsomal preparations (Liu and Coughtrie, 2017; Soars, 2002). The exact mechanism of this phenomenon, generally referred to as UGT latency, has not been explicitly elucidated. However, it has been reported that ER preparations, such as liver microsomes, show increased UGT activities if the microsomal membrane is physically or chemically disrupted, e.g., with the pore-forming agent alamethicin or surfactants, respectively (Liu and Coughtrie, 2017). Although intact hepatocyte cultures often better predict the *in vivo* clearance of UGT substrates (Engtrakul et al., 2005; Soars et al., 2002), the microsomal preparations are more feasible for mechanism-based drug metabolism studies and differentiating metabolic interactions from other cellular processes, such as drug permeation.

In this study, we developed a microfluidic reactor, incorporating immobilized human liver microsomes (HLM), for studying UGT metabolism under flow-through conditions and shedding light on the mechanisms of UGT latency. Namely, conducting enzyme incubations under flow-through conditions allows time-resolved monitoring of the enzyme function, such as distinguishing between transient and steady-state reaction velocities, which facilitates mechanistic studies in ways not feasible for conventional (static) endpoint assays. In previous studies, a range of different protocols have been proposed for immobilization of CYPs on both capillary-based and microfabricated reactors (Kiiski et al., 2019; Lee et al., 2013; Nicoli et al., 2008; Schejbal et al., 2016), but prior research on UGT metabolism under flow-through conditions is limited to only a handful of studies exploiting capillary-based approaches (Alebić-Kolbah and Wainer, 1993; Kim and Wainer, 2005; Sakai-Kato et al., 2004). In this study, we exploited modern microfabrication techniques to realize microreactors featuring a precisely confined micropillar array as the solid support for the immobilization of HLM. Compared with packed-bed capillary reactors, the microfabricated pillar arrays enable better control over the total surface area for enzyme immobilization, and they are less prone to clogging compared with, for example, porous polymer monolith-based reactors (Munirathinam et al., 2015). Microfabrication also enables much better multiplexing and integration possibilities than capillary systems (Suryawanshi et al., 2018) and thus creation of microchannel networks that enable precise spatiotemporal control over drug concentrations.

2. Material and methods

2.1. Materials and reagents

The monomers used for fabricating the microreactors, pentaerythritol tetrakis(3-mercaptopropionate) ('tetrathiol') (≥95.0%) and triallyl-1,3,5-triazine-2,4,6(1H,3H,5H)- trione ('triallyl') (≥98.0%), were purchased from Sigma-Aldrich (Saint Louis, MO) or Bruno Bock (Marschacht, Germany). The microfabricated masters were made using SU-8 100 (Micro Resist Technology, Berlin, Germany) and the poly (dimethylsiloxane) (PDMS) molds were prepared from Sylgard 184 elastomer (Down Corning Corporation, Midland, MI).

The reagents used for functionalization of the microreactor surface included biotin-PEG_4-alkyne and ethylene glycol purchased from Sigma Aldrich (St. Louis, MO), Irgacure® TPO-L photoinitiator from BASF (Ludwigshafen, Germany), and streptavidin Alexa Fluor® 488 conjugate from Life Technologies (Eugene, OR). The lipids used for preparation of fusogenic liposomes were purchased from Avanti Polar Lipids (Alabaster, AL) and included 1,2-dioleoyl-3-trimethylammonium-propane (chloride salt) (DOTAP), 1,2-dioleoyl-*sn*-glycero-3-phosphoethanolamine (DOPE), 1,2-dioleoyl-*sn*-glycero-3-phosphoethanolamine-N2 (cap-biotinyl) (sodium salt) (biotin-cap-DOPE) and 1,2-dioleoyl-*sn*-glycero-3-phosphoethanolamine-N-(lissamine rhodamine B sulfonyl) (ammonium salt) (lissamine rhodamine B-DOPE).

The human liver microsomes (HLM, 20 donor pool, Corning® Gentest #452161, Lot 7331001) were purchased from Corning (Wiesbaden, Germany). The chemicals and reagents used in the enzyme incubations included 8-hydroxyquinoline (8-HQ), 8-hydroxyquinoline-glucuronide, magnesium chloride hexahydrate, perchloric acid ($HClO_4$), uridine 5'-diphosphoglucuronic acid trisodium salt (UDPGA), alamethicin, bovine serum albumin (BSA), Trizma® base and phosphate-buffered saline (PBS, pH 7.4), all purchased from Sigma Aldrich. Zidovudine and zidovudine glucuronide were from Toronto Research Chemicals (North York, ON). All chemicals used in the study were of analytical grade unless otherwise stated. Water was purified with MilliQ water purification system (Millipore, Molsheim, France).

2.2. Biotinylation of human liver microsomes

To enable immobilization of HLM on streptavidin-functionalized microreactor surfaces, the HLM were first biotinylated off-chip by spontaneous fusion between biotin-tagged fusogenic liposomes (b-FL) and the HLM, following a previously developed protocol (Kiiski et al., 2019). The b-FL were prepared by mixing chloroform solutions of DOPE (10 mg/mL), DOTAP (10 mg/mL), biotin-cap-DOPE (10 mg/mL), and lissamine rhodamine B-DOPE (1 mg/mL) lipids in a mass ratio of 1:1:0.1:0.05. After evaporating the solvent under nitrogen gas, the dry lipids were kept in vacuum for 2 h to remove any residual solvent before resolvating the dry lipid film in PBS buffer. This yielded large multilamellar liposomes with a total lipid concentration of 2 mg/mL. To ensure complete solvation, the lipid dispersion was vortexed for 1 h at room temperature after which the large multilamellar liposomes were extruded through a porous polycarbonate membrane (pore size of 0.1 μm) to yield large unilamellar vesicles (220 ± 25 nm, n=4 batches) with fusogenic properties, i.e., the b-FL. Finally, the b-FL (2 mg/mL lipid concentration in PBS) and the commercial HLM (20 mg/mL total protein in 250 mM sucrose) stock solutions were mixed in equal volumes and incubated at 37°C for 15 min to yield the biotinylated HLM (b-HLM) solution with 10 mg/mL total protein concentration.

2.3. Microreactor fabrication and biofunctionalization

The microreactors were made of off-stoichiometric thiol-enes (OSTE) and incorporated a 30 × 4 × 0.2 mm (length × width × height) micropillar array featuring ca. 14 400 pillars (Ø 50 μm) in a hexagonal lattice with interpillar (center-to-center) distance of 100 μm and a total effective volume of ca. 18.3 μL (Fig. 1A and B). The manufacturing protocol consisted of four steps: (i) microfabrication of SU-8 masters of the micropillar and cover layers, (ii) soft lithography of the PDMS molds of the micropillar and cover layers with the assistance of the SU-8 masters, (iii) UV replica molding of the micropillar and cover layers in OSTE with the assistance of the PDMS molds, and (iv) bonding of the OSTE micropillar and cover layers to obtain a sealed micropillar channel. The SU-8 master (step i) was fabricated by photolithography, similar to Kiiski et al. (2019). The PDMS molds (step ii) were prepared by mixing the Sylgard 184 base elastomer and the curing agent in a weight ratio of 10:1, degassing the mixture under vacuum for 30 min, and curing in the oven against the SU-8 masters (either at 80°C for 3 h or 65°C overnight). The OSTE layers were prepared by mixing the tetrathiol and triallyl monomers in a ratio yielding 25% molar excess of thiol functional groups. The monomer mixture was then poured onto the PDMS mold, degassed under vacuum for ca. 5 min, and cured under UV for 5 min (Dymax 5000-EC Series UV flood exposure lamp, nominal power 225 mW/cm^2, Dymax Corporation, Torrington, CT). After curing, the OSTE micropillar and cover layers were laminated against each other (step iv) and the bonding was finalized with an additional UV exposure through the cover layer for 2 min (Dymax 5000-EC). The structural fidelity of the OSTE-based micropillar arrays was examined by scanning electron microscopy (Quanta™ 250 FEG, FEI, Hillsboro, OR) using a platinum coating (ca. 5 nm coating thickness).

Next, the microreactor surface was functionalized step-wise with

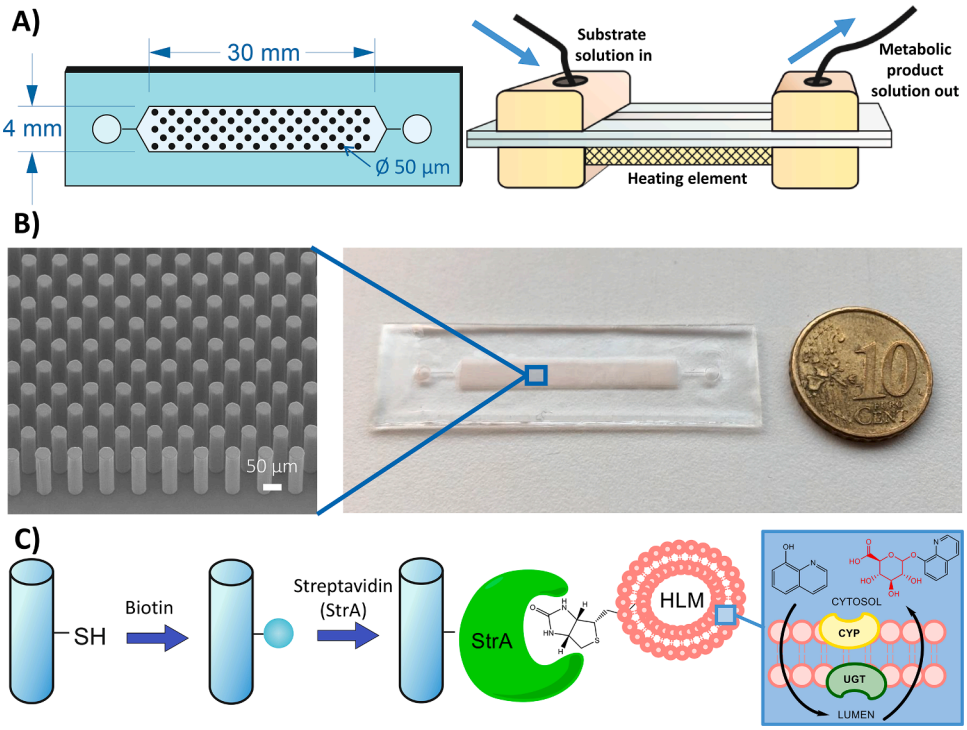

Fig. 1. Overview of the microreactor layout. A) A schematic top view of the microreactor with annotated dimensions and a schematic side view of the experimental setup. B) A scanning electron microscopy (SEM) detail of the micropillar array and a photograph of the microreactor. C) Schematic view of the enzyme immobilization and reactor functionalization protocols with a graphical illustration (insert on the right) of a typical UGT-mediated glucuronidation reaction occurring on the luminal side of the ER membrane.

biotin and streptavidin before immobilization of the b-HLM (Fig. 1C). First, the thiol-rich microchannel was filled with biotin-PEG$_4$-alkyne (0.1 mM in ethylene glycol, with 1% Irgacure® TPO-L) and exposed to UV through the cover layer for 1 min (λ = 365 nm, LED, nominal intensity 14 mW/cm^2) to initiate the reaction between the surface thiols and the alkyne. After this initial biotinylation step, the microchannel was rinsed sequentially with methanol and water (≥5 mL each). Then, the microchannel was coated with streptavidin (0.5 µg/mL in PBS) via incubation at room temperature (RT) for 30–45 min, and rinsing with ≥5 mL PBS. Finally, the prebiotinylated HLM (b-HLM) was immobilized onto the micropillars by filling the streptavidin-coated microchannel with b-HLM solution (10 mg/mL, prepared as described above), and incubating at 4 °C overnight. To avoid evaporation of the b-HLM solution, the microchannel inlet and outlet were sealed with Parafilm®. Before use, the microreactor was rinsed with ≥5 mL of the incubation buffer to remove the excess (non-immobilized) b-HLM. The average amount of the immobilized b-HLM was equivalent to 0.021 ± 0.010 mg total microsomal protein (n=4 microreactors). The amount of the immobilized b-HLM was determined by measuring the total protein concentration of the rinse solution (after b-HLM immobilization) with the Pierce™ BCA Protein Assay Kit (Thermo Fischer Scientific, Rockford, IL) and comparing its protein concentration with that of the filling solution (b-HLM, 10 mg/mL total protein).

2.4. Microfluidic drug glucuronidation assays

The UGT activity of immobilized HLM was determined by feeding the substrate (either 8-hydroxyquinoline (8-HQ) or zidovudine) and the cosubstrate (1 mM UDPGA), both dissolved in Tris buffer (0.1 M, 5 mM $MgCl_2$, pH 7.5), through the reactor at a constant volumetric flow rate of 5 µL/min. As the volume of the micropillar array was ca. 18.3 µL, this corresponds to a residence time of 3.7 min. The enzyme stability was determined using a constant concentration of the substrate (50 µM 8-HQ) and other reagents and an external syringe pump (one pump configuration). The impact of residence (reaction) time on the metabolite yield was additionally determined between 1.2 min (15 µL/min) and 7.3 min (2.5 µL/min) by adjusting the flow rate of the feed solution accordingly. For enzyme kinetic determinations (zidovudine glucuronidation), a two-pump configuration was used so that one pump line was feeding constant concentration of the substrate and the cosubstrate (6000 µM zidovudine, 1 mM UDPGA) and the other pump line only the cosubstrate (1 mM UDPGA). These two feed solutions were mixed off-chip, with the help of a three-way T-piece tubing connector, before introducing the combined flow to the microreactor. The two pump lines were programmed so that the total combined flow rate remained unchanged (5 µL/min) during the experiment, but the relative share of the substrate solution varied from 1% (equivalent to 60 µM zidovudine) to 100% (equivalent to 6000 µM zidovudine) of the total volumetric flow.

All microreactor experiments were conducted at physiological temperature (ca. 37°C) by placing an aluminum heating element under the reactor (Fig. 1A). The heating power was adjusted automatically using a PID controller employing a thermocouple (both from Omega Engineering Inc., Stamford, CT) attached to the top of the microreactor cover layer and adjusted to 35 °C, assuming ca. 2 °C difference between the top surface and the inside temperature on the basis of the previous study (Sikanen et al., 2008). The impacts of alamethicin (50 µg/mL) or bovine serum albumin (0.1%, m/v) on UGT activity under flow-through conditions were determined by adding these to the feed solution, where indicated. Additionally, the impact of alamethicin on the UGT activity was determined by preincubating the microreactor with alamethicin (500 µg/mL in Tris buffer) at 4°C for 30 min before initiating the flow-through experiment.

The amounts of the produced metabolites were quantitated by fluorescence (8-hydroxyquinoline glucuronide) or liquid chromatography-mass spectrometry (LC-MS, zidovudine glucuronide) from 50 µL fractions of the output solution collected using a refrigerated fraction collector (CMA 470, CMA Microdialysis AB, Solna, Sweden). For fluorescence analysis (ex/em 245/475 nm), the 50 µL fractions were diluted 1:1 with Tris buffer, acidified with 10 µL of 4 M $HClO_4$, and analyzed with a Varioskan LUX well plate reader (Thermo Scientific, Vantaa Finland). For mass spectrometric (MS) analysis, the 50 µL fractions were diluted 1:1 with acetonitrile and analyzed using an ACQUITY UPLC™ liquid chromatograph (Waters, Milford, MA) and Xevo TQ-S triple quadrupole mass spectrometer (Waters, Manchester, UK). The

LC-MS data were analyzed using MassLynx V4.1 software. The chromatographic and MS parameters and method validation results for zidovudine glucuronide quantitation are provided in the Supplementary material (Tables S1-S2 and Figure S1). The enzyme activities in flow-through conditions were calculated by dividing the metabolite concentration of the outcome with the residence time (dependent on the flow rate) and the amount of the immobilized HLM (0.021 ± 0.010 mg total microsomal protein). To allow comparison with static incubations, these enzyme activities (μM/min/mg protein) were multiplied with the reaction volume of the static enzyme incubations (100 μL) to balance the initial amount of the substrate and thus obtain same unit activities (pmol/min/mg protein).

2.5. Determination of drug glucuronidation in static enzyme incubation conditions

The control UGT activities in non-immobilized HLM were determined in sample tubes using a total volume of 100 μL, and a total protein concentration of 0.2 mg/mL (8-HQ incubations) or 0.1 mg/mL (zidovudine incubations) in Tris buffer (0.1 mM, 5 mM $MgCl_2$, pH 7.5). Where indicated, the HLM preincubation with alamethicin (50 μg/mL) was first conducted at 4 °C for 30 min. The HLM and the substrate were further preincubated at 37°C for 5 min before initiating the reaction by the addition of the cosubstrate (UDPGA, 1 mM). The substrate concentrations were either 50 μM (8-HQ) or between 25 and 6400 μM (zidovudine, enzyme kinetic determinations). After the desired incubation time (10 min for 8-HQ and 30 min for zidovudine), the reactions were terminated by the addition of 10 μL of 4 M $HClO_4$, the solutions kept on ice for 20 min, and centrifuged at 16 000 g for 10 min to precipitate the enzymes. The supernatants were analyzed by fluorescence (8-HQ incubations) or LC-MS (zidovudine incubations), similar to the fractions collected from the microreactors. The enzyme activities in static conditions were calculated by dividing the metabolite amount produced (pmol) with the amount of HLM (mg total microsomal protein) and the reaction time.

The impacts of the tetrathiol or triallyl monomers used in the microfabrication, and possibly leaching out of the bulk polymer, on the activity of 8-HQ glucuronidation were additionally examined in static conditions by adding either of the monomers to the incubation buffer at concentrations between 0.01 and 1000 μM (Supplementary material, Figure S2).

2.6. Statistics

All results are presented as mean ± standard deviation from repeated experiments, the number of which is indicated in the context of each dataset. Enzyme kinetic parameters were calculated by fitting the experimental data to the Michaelis-Menten equation. Statistical difference between kinetic parameters (K_M, V_{MAX}) were evaluated using the extra sum-of-squares F-test. Other statistical analyses were performed using the Student's t-test using 95% confidence interval criteria, i.e., $p<0.05$ for statistically significant difference. All statistical analyses and curve fittings were performed using GraphPad Prism version 8.4.3 (GraphPad Software, San Diego, CA).

3. Results and discussion

3.1. Impact of biotinylation and immobilization on the microsomal UGT activity

Microreactor performance was initially characterized using 8-hydroxyquinoline, a substrate metabolized by several UGTs to yield a fluorescent metabolite, 8-hydroxyquinoline glucuronide, which can be selectively quantified by fluorescence (Smith, 1953). The HLM immobilization approach exploited in this study is based on biotinylation of the microsomal membranes upon their spontaneous fusion with biotin-containing fusogenic liposomes. Since the functionalization method does not target the protein structure, but the surrounding lipid membrane, it is unlikely to affect the enzyme function similar to immobilization strategies based on covalent bonding between the protein and the solid support, which represent the majority of previous work (Sheldon, 2007). Furthermore, when the biotinylated HLM is immobilized on an avidin-coated micropillar array, the system is scaffold-free, and the HLM remains accessible to the UGT substrates and cosubstrate (UDPGA) so that the enzyme kinetic determinations are not impaired by the system-restricted mass transfer typically associated with scaffold-based systems (i.e., enzymes entrapped in porous matrices (Sheldon, 2007)). However, the fusion process inevitably results in alterations in the lipid composition of the microsomal membrane, which may have an impact on the diffusion of UGT substrates and cosubstrate to the luminal side of the membrane or result in conformation changes in the protein structure due to lipid-protein interactions. These are both critical processes affecting the kinetics of UGT-catalyzed reactions *in vitro* (Hochman et al., 1981; Palaiokostas et al., 2018; Vessey and Zakim, 1971).

To examine the impact of the HLM biotinylation (fusion) process on the apparent UGT activity, we first determined the 8-HQ glucuronidation rate in native and biotinylated HLM under static conditions (in sample tubes) and compared the obtained activity with that of alamethicin-pretreated HLM (Fig. 2A and B). Preincubation of HLM with alamethicin, and the subsequent pore formation in the microsomal membrane, is currently considered the gold standard to overcome UGT latency, and typically preferred over the use of surfactants, which show much narrower concentration dependency (Fisher et al., 2000). In this study, a statistically significant ($p = 0.02$, Student's t-test) increase in the UGT activity was observed in biotinylated HLM with approximately 25% greater activity over native HLM in static conditions (Fig. 2B). The observed increase in the UGT activity may be explained, for instance, by the relative increase of long-chain fatty acids, which has been reported to elevate UGT activity (Hochman et al. 1981), or by the introduction of non-lamellar DOPE into the microsomal membrane, which has been reported to promote membrane permeation of small molecules (Palaiokostas et al., 2018). The observed activity increase was, however, negligible compared with that achieved by alamethicin preincubation (Fig. 2B), suggesting that biotinylation does not result in a similar physical membrane disruption as alamethicin-induced pore formation. In static conditions, the synergistic impact of biotinylation (membrane fusion) and alamethicin preincubation (pore formation) was statistically insignificant compared with that of alamethicin alone (Fig. 2B). On this basis, it was concluded that although the biotinylation (fusion) process exploited in this study alters the membrane composition, it preserves the UGT activity somewhat close to that of the intact HLMs. Overall, these results are consistent with the 'compartmentalization hypothesis' (Liu and Coughtrie, 2017), which is the most widely accepted theory suggesting that the UGT latency is best explained by the diffusion-limited, impaired mass transfer of the UGT substrates and cosubstrate through the microsomal membrane *in vitro*. In static conditions, the diffusion rate thus delimits the maximal reaction rate unless the diffusional restrictions are eliminated, for instance, with the help of alamethicin induced pore formation.

When immobilized onto the microreactor surface, the UGT activity of b-HLM was shown to be highly stable over time, with a negligible decrease in enzyme activity within the first 10 h of continuous use, and a rather minor decrease during the subsequent 5 h period (Fig. 2C). The within-run variation (n=6 subsequent fractions, each 50 μL) determined for 8-HQ glucuronidation at a flow rate of 5 μL/min was between 0.7 and 7.4% RSD (for n=4 individual microreactors) and the chip-to-chip variation of the average activities was 21.0% RSD. Further validation of the flow-through UGT assays confirmed that the UGT activity of the immobilized HLM was dependent on the reaction temperature, as expected, similar to that of non-immobilized native HLM in static conditions (Figure 2D). Overall, these results confirmed that the membrane

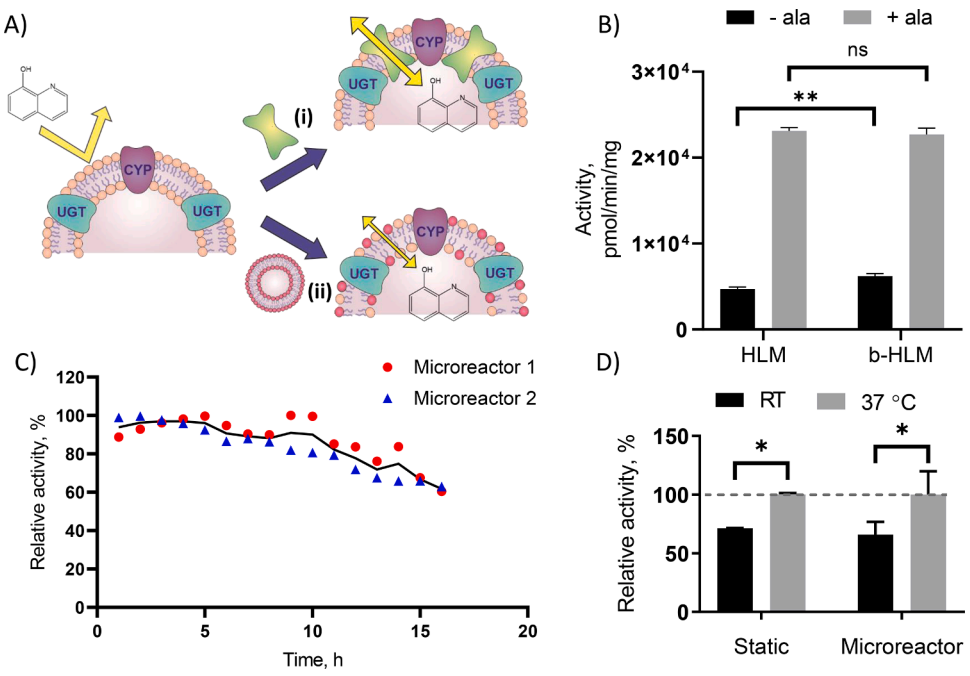

Fig. 2. Characterization of the UGT enzyme activity and stability. A) A schematic visualization of the effects of (i) alamethicin and (ii) liposome fusion on the membrane structure and permeability of human liver microsomes. B) The effect of alamethicin (ala) on the 8-HQ glucuronidation rate in non-immobilized native HLM and biotinylated HLM (b-HLM) when the enzyme incubation is conducted in sample tubes (à 100 µL) in static conditions. The error bars represent the variation between n=3 individual incubations. C) The stability of the UGT activities of two parallel microreactors featuring immobilized HLM over a 15-hour-long experiment at a flow rate of 2.5 µL/min. Activity presented as % of maximal activity of each microreactor. D) The effect of temperature on UGT activity under static (soluble HLM, n=3 incubations each) and flow-through conditions (n=4 microreactors, 2.5 µL/min). 8-hydroxyquinoline was used as the probe substrate at a concentration of 50 µM in all experiments.*p-value < 0.05, **p-value < 0.005 (Student's t-test). n.s. = not significant.

biotinylation and subsequent immobilization of the b-HLM is a robust protocol and does not result in enzyme inactivation or leaching of the immobilized enzymes out of the microreactor along with the applied flow. It was also confirmed that neither of the monomers used in the fabrication of the microreactors resulted in any kind of enzyme inhibition up to at least 1 mM concentration (Supplementary material, Figure S2). Thus, the UGT activity was concluded unaffected by chemical artifacts possibly originating from the microreactor manufacturing process.

3.2. *Impact of flow-through conditions on the determination of microsomal UGT activity*

In addition to enzyme stability, the mass transfer in flow-through conditions merits special attention. Upon diffusion of the reaction components across the immobilized HLM membrane, the flow-through system eventually reaches a steady state, resulting in a plateau level of UGT activity (Fig. 3A). In this study, the impact of alamethicin pore formation on the maximum achievable glucuronidation activity in flow-through conditions was examined using 8-HQ as the model substrate and two different approaches for alamethicin treatment, including (i) pre-incubation of the microreactor with alamethicin (500 µg/mL in Tris buffer, 30 min, 4°C) before initiation of the experiment and (ii) addition of alamethicin (50 µg/mL) to the feed solution during the experiment (Fig. 3A). At high flow rates (here, 15 µL/min corresponding to residence time of 1.2 min), similar increase in the absolute 8-HQ glucuronidation activity was observed with alamethicin, as in the case of static assays (Fig. 3A vs. 2B). Preincubation of the microreactor with alamethicin enabled elimination of diffusional restrictions and readily resulted in about two-fold greater UGT activity compared with the plateau level activity of microreactors not treated with alamethicin. By adding alamethicin to the feed solution, even a greater increase in the UGT activity (ca. three-fold) was achieved as soon as the steady-state was reached within about 15 min (Fig. 3A). However, in addition to alamethicin, the flow rate has huge impact on the steady-state formation under flow-through conditions, as it controls the residence time of the substrate within the system. Thus, the flow rate affects the equilibrium of the substrate concentration in the cytosolic and luminal sides of the immobilized HLM and its impact must also be accounted for when deriving enzyme kinetic constants from flow-through experiments.

In this study, the impact of the residence time on the UGT activity was determined by quantitating the metabolite concentration from 50 µL fractions of the feed solution, run through the microreactor and analyzed off-chip by fluorescence. This volume was considered the most feasible for further handling to ensure adequate sample manipulation accuracy. However, the time required for the fraction collection (à 50 µL) is also proportional to the flow rate and varies between 3.3 min (15 µL/min) and 20 min (2.5 µL/min) with the flow rates used in this study. In practice, this means that at the highest flow rate (15 µL/min), 3-4 dummy fractions need to be collected before the steady state condition is reached (t=15 min and onward), as is illustrated with the help of 8-HQ glucuronidation in Fig. 3A. At the lowest flow rate (2.5 µL/min), the fraction collection takes 20 min and already the second fraction is thus representative of the UGT activity of the steady state. However, comparison of the fraction-specific activities at different flow rates, in the absence of (Fig. 3B) and with alamethicin in feed solution (Fig. 3C), revealed that, as the residence time of the substrate increased (i.e., the flow rate decreased), the accelerating impact of alamethicin became negligible. Further comparison of the amounts of metabolite produced per fraction, at conditions representative of the steady-state at each flow rate, confirmed that the reaction was not diffusion-limited as the amount metabolite increased linearly as a function of residence time in both cases (Fig. 3D). However, in the absence of alamethicin, the metabolite production rate (pmol per residence time) was somewhat higher compared with that of alamethicin-treated microreactors, and reached saturation at residence times t>3-4 min (Fig. 3D). Assuming maximum UGT activity of about 4 µM/min (Fig. 3B), the residence times beyond 4 min yield >16 µM metabolite concentrations, which correspond to >32% conversion of the substrate (50 µM 8-HQ) to its respective metabolite. Thus, the results suggest that the flow-through reaction obeys Michaelis-Menten type kinetics, in which excessive substrate depletion results in concentration-dependent first-order kinetics and thus, reduced reaction velocity. Instead, with alamethicin in feed, the metabolite amount increased linearly over residence time at all flow rates tested, only at a somewhat lower rate (pmol per residence time) compared with microreactors not treated with alamethicin (Fig. 3D).

The apparent difference in the alamethicin impact between the static assays (Fig. 2B) and the flow-through microreactor assays (Fig. 3D) may

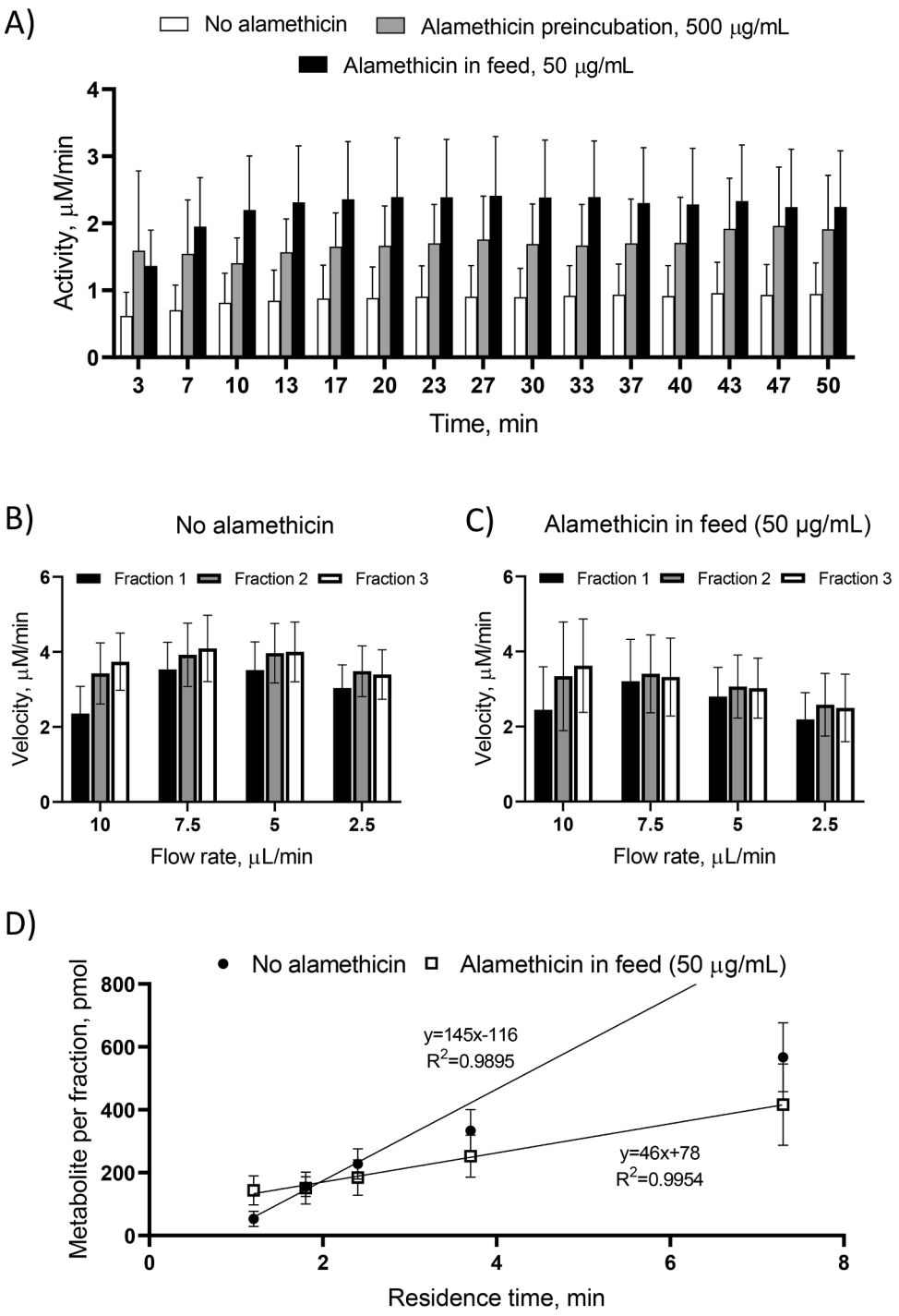

Fig. 3. The alamethicin effect on UGT activity of immobilized HLM in flow-through conditions. A) The impact of alamethicin on the steady-state formation time in a microreactor operated at a flow rate of 15 uL/min. Data point frequency is one every 3.3 min for collection of 50 μL fractions. The error bars represent the deviation between n=4 microreactors in each case. B-C) UGT activity in subsequent fractions 1–3 (each 50 uL) collected from the microreactor at different flow rates in the absence (B) and presence of alamethicin (C). The error bars represent the deviation between n=4 (without alamethicin) and n=4 (with alamethicin) microreactors. D) The impact of residence time on the amount of 8-HQ-glucuronide produced per fraction on microreactors in the absence of alamethicin and with alamethicin included in the feed solution (50 μg/mL). The error bars represent the deviation between n=4 microreactors in each case.

be explained by the inherent differences in the quantitation of the metabolite amount between static and flow-through experiments. The results derived from static assays always represent the cumulative amount of the produced metabolite over the entire reaction time, and thus, in the absence of alamethicin, they reflect the average of the initial and steady-state reaction velocities. Instead, the flow-through assays are capable of revealing the transient activity so that the steady-state velocity can be distinguished from the initial velocity, as illustrated in Fig. 3A. Thus, on the basis of the microreactor experiments, it may be concluded that if only the residence time of the substrate is long enough to reach equilibrium between the cytosolic and luminal concentrations, the enzymatic reaction proceeds with constant velocity, so that the amount of the metabolite produced is dependent on the reaction time, but independent of alamethicin (pores). Furthermore, our results further hint at even somewhat greater UGT activity in the absence of alamethicin (Fig. 3D). Explaining the exact mechanism of this finding would warrant further studies beyond the scope of this paper, but it may be hypothesized that the artificial alamethicin pore in the HLM membrane shifts the equilibrium of the enzyme-substrate complex formation (E+S⇌ES) toward the reverse dissociation. As a result, the concentration of the ES complex in the lumen may decrease and result in reduced metabolite formation rate (ES→E+M) compared with the situation in intact microsomes. To be able to compare these reaction velocities with those of the static assays, the maximum steady-state 8-HQ glucuronidation activities measured on microreactors (in μM/min, Figs. 3B and C) were divided by the amount of the immobilized HLM (0.021±0.010

mg total protein) and multiplied with the reaction volume of the static assays (100 µL) so as to equalize the initial amount of the substrate. The so obtained activities were 1.95±0.42 × 10^4 pmol/min/mg protein in the absence of alamethicin and 1.58±0.49 × 10^4 pmol/min/mg protein with alamethicin in feed, both determined at a flow rate of 7.5 µL/min (n=4 microreactors each). These values correlated well with the 8-HQ glucuronidation activity in the static assays with alamethicin (2.31±0.03 × 10^4 pmol/min/mg protein, n=3 incubations) and were substantially greater than those measured in the static conditions in the absence of alamethicin (Fig. 2B).

Overall, these observations are consistent with the compartmentalization hypothesis, according to which the apparent increase in reaction velocity observed in the presence of alamethicin in static endpoint assays is not due to intrinsic changes in UGT activity but the elimination of mass transfer barriers. However, in flow-through conditions, the steady-state velocity can be distinguished from the initial (diffusion-limited) velocity and thus the use of alamethicin does not confer any substantial advantages. As the use of alamethicin on microreactors also resulted in a slightly higher chip-to-chip variation (Figs. 3B-C), it was excluded from all subsequent enzyme kinetic experiments.

3.3. Determination of in vitro intrinsic clearances under flow-through conditions

Enzyme inhibition caused by free fatty acids released from artificial microsomal preparations, that affect both CYPs and UGTs alike (Palacharla et al., 2017; Rowland et al., 2007), is an alternative theory to explaining the underestimation of drug clearance in isolated microsomal preparations *in vitro*. Typically, elimination of the fatty acid artifacts is achieved by adding albumin to the *in vitro* enzyme incubations. A well-known target of fatty acid-induced inhibition is UGT2B7, which is responsible for the glucuronidation of ca. one-third of marketed drugs (Williams et al., 2004), making it one of the clinically most important UGT enzymes. Zidovudine is a specific UGT2B7 substrate, whose *in vivo* clearance is significantly underestimated based on *in vitro* data (Boase and Miners, 2002) unless albumin is added to the *in vitro* enzyme incubations. To further evaluate the feasibility of the flow-through microreactor technology for predicting the *in vivo* clearance of therapeutic drugs, we determined the enzyme kinetic parameters (K_M and V_{MAX}) of zidovudine in the presence and absence of albumin. Although albumin may also change the free unbound concentration of the test substrate, binding of zidovudine to albumin is negligible and the albumin effect has been associated with sequestering of the free fatty acids, which eventually results in a substantial increase in the *in vitro* intrinsic clearance of zidovudine (Manevski et al., 2011; Rowland et al., 2007). This effect was also examined in our own experiments with and without alamethicin in static conditions (Fig. 4A) as well as on microreactors not treated with alamethicin (Fig. 4B). To examine the impact of albumin on the zidovudine glucuronidation kinetics in flow-through conditions, we used an interconnected two-pump configuration, which enabled the creation of a concentration gradient covering ca. two orders of magnitude (60–6000 µM zidovudine). At each zidovudine concentration, three subsequent fractions, each 50 µL, were collected at a flow rate of 5 µL/min (residence time of 3.7 min). Despite the considerable difference in the partition coefficients between zidovudine (log*P* ≈ 2) and 8-HQ (log*P* ≈ 0.05), the time required for steady-state formation and reaching the equilibrium between the cytosolic and luminal substrate concentrations was comparable in both cases (Supplementary material, Figure S3). Thus, to ensure that the system had reached the steady state, the kinetic constants were determined using the glucuronide amount of the last of the three fractions collected at each zidovudine concentration. On the basis of the microreactor characterization conducted with the help of 8-HQ glucuronidation, alamethicin was excluded from the flow-through microreactor experiments with zidovudine.

In the absence of albumin, the enzyme affinity (K_M) of zidovudine glucuronidation in static assays increased upon addition of alamethicin, whereas the K_M derived from microreactor experiments was between these two values (Fig. 4C). However, the maximal activity (V_{MAX}) derived from microreactor experiments was somewhat larger compared with that of static assays conducted with and without alamethicin (Fig. 4D), which resulted in a statistically similar intrinsic clearance (CL_{int}) as that of the static assays conducted with alamethicin (Fig. 4E).

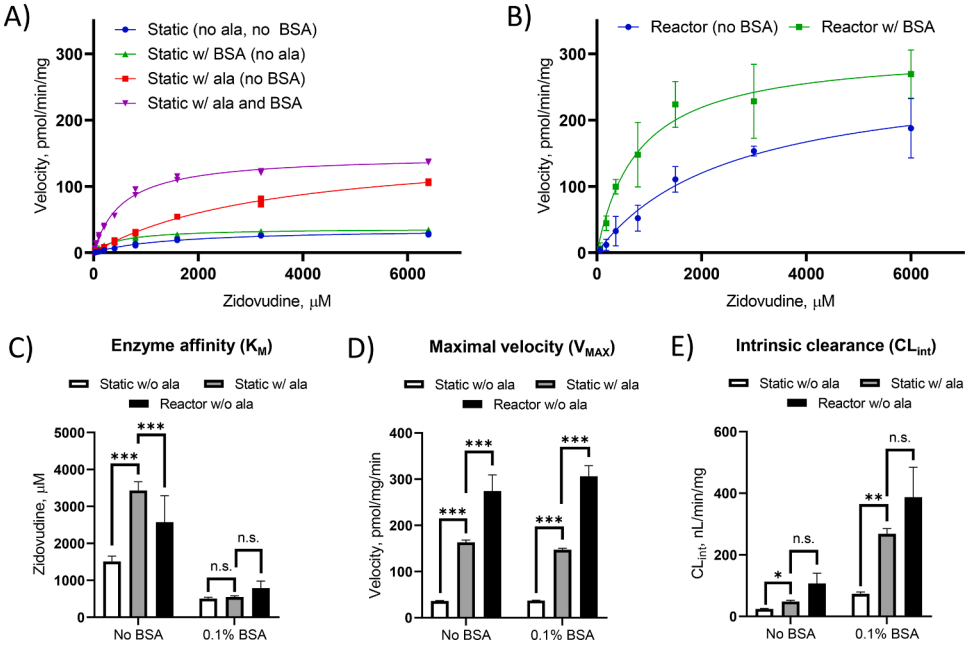

Fig. 4. Comparison of zidovudine glucuronidation kinetics in static and flow-through conditions. Michaelis-Menten kinetics determined for zidovudine glucuronidation using A) static, endpoint incubations, and B) microreactors not treated with alamethicin. In static assays, the samples were assayed in duplicate with and without bovine serum albumin (BSA, 0.1 % w/v) and/or alamethicin (ala, 50 µg/mL). For the microreactors, the error bars represent the deviation between n=3 microreactors for which the zidovudine glucuronidation rate was determined with and without BSA (0.1 % w/v) by quantitating the metabolite from the third fraction (à 50 µL) collected at each concentration. The zidovudine concentration gradient was created by feeding 6000 µM zidovudine in the incubation matrix (0.1 M Tris, 5 mM $MgCl_2$, 1 mM UDPGA) from one syringe and the blank incubation matrix from another syringe and mixing these appropriately by adjusting the ratio of the two flows while maintaining a total flow rate of 5 µL/min (3.7 min residence time) over the entire duration of the experiment. Summaries of C) the enzyme affinities, D) maximal enzyme activities, and E) intrinsic clearances obtained for zidovudine glucuronidation in static and flow-through conditions. **p*-value < 0.05, ***p*-value < 0.005, ***p-value < 0.0005 (Student's t-test). n.s. = not significant.

Supplementing the enzyme incubations with purified bovine serum albumin resulted in a clear decrease in the K_M values derived from both static and microreactor experiments (Fig. 4C), but it did not much impact the V_{MAX} values (Fig. 4D). In static conditions, the V_{MAX} was mostly impacted by alamethicin preincubation, whereas the V_{MAX} values derived from microreactor experiments were statistically similar with and without albumin (Fig. 4D). As expected based on previous literature, the combined impact of alamethicin and albumin in static conditions resulted in approximately 11-fold increase in the intrinsic clearance (V_{MAX}/K_M) of zidovudine, from 24±2 nL/min/mg protein in intact HLM to 268±17 nL/min/mg protein with alamethicin and albumin (Fig. 4E). The intrinsic clearance derived from microreactor experiments, supplemented with albumin, was 390±100 nL/min/mg protein and thus statistically similar with that of the static assays conducted in the presence of both albumin and alamethicin (Fig. 4E). As the flow effectively removes any soluble fatty acid artifacts from the cytosol side of the immobilized microsomal membrane, these results suggest that the inhibitory fatty acid artifacts are likely accumulated on the luminal side as well, and albumin helps sequester the fatty acids upon their partitioning across the microsomal membrane. These results also suggest that conducting drug glucuronidation assays under flow-through conditions could likely improve the *in vitro-in vivo* extrapolation of drug clearance compared with intact microsomes, without needing to use artificial membrane-disruptive agents such as alamethicin.

4. Conclusions

A microfluidic reactor incorporating immobilized human liver microsomes was introduced to the study of UGT-mediated drug metabolism under flow-through conditions. The microreactor was characterized with respect to key performance parameters, including temperature-dependency and long-term stability. The decrease in enzyme activity within the first 10 h of continuous use at 37 °C was less than 20%. We also confirmed that the materials used in the microreactor fabrication did not interfere with UGT metabolism. In addition, the governing principles for the determination of enzyme kinetic parameters under flow-through conditions were drawn to examine UGT metabolism in general and to shed light on the latency associated with UGT assays *in vitro* via alamethicin and albumin effects. In flow-through conditions, alamethicin was shown to have a negligible impact on the drug clearance, whereas the albumin effect (fatty acid sequestering) was similarly reproduced in flow-through and static conditions. As a result, the kinetics of zidovudine glucuronidation (the model reaction used in this study) under flow-through conditions was in good agreement with that obtained using microsomal incubations supplemented with alamethicin and albumin. Considering the possibility to re-use a single microreactor continuously for at least 10 h without significant loss of UGT activity, the theoretical maximum number of samples (à 50 μL) collected, for example, at a flow rate of 5 μL/min (à 10 min per aliquot), is as high as sixty. This suffices for, e.g., determination of the enzyme kinetic parameters of two-three drug compounds per a single microreactor, assuming that minimum of three representative aliquots are collected at six or more different drug concentrations for each compound. Furthermore, our results suggest that conducting drug glucuronidation assays under flow-through conditions may shed light on the mechanism-based UGT studies by enabling new designs of experiments not feasible for static enzyme incubations, such as time-resolved studies of enzyme function and creation of time-dependent concentration gradients of the substrates, cosubstrates or inhibitors.

CRediT authorship contribution statement

Iiro Kiiski: Conceptualization, Methodology, Investigation, Validation, Formal analysis, Writing - original draft. **Elisa Ollikainen:** Methodology, Writing - review & editing. **Sanna Artes:** Investigation. **Päivi Järvinen:** Supervision, Writing - review & editing. **Ville Jokinen:** Supervision, Writing - review & editing. **Tiina Sikanen:** Supervision, Writing - review & editing, Conceptualization, Project administration, Funding acquisition.

Acknowledgements

This work was financially supported by the Academy of Finland (grants 309608, 314303, 308911) and the Doctoral Programme in Drug Research, Doctoral School in Health Sciences, University of Helsinki. The Electron Microscopy Unit of the Institute of Biotechnology, University of Helsinki is acknowledged for providing access to the scanning electron microscope, and the DDCB core facility, University of Helsinki and Biocenter Finland, for providing access to the plate reader.

Supplementary materials

Supplementary material associated with this article can be found, in the online version, at doi:10.1016/j.ejps.2020.105677.

References

Alebić-Kolbah, T., Wainer, I.W., 1993. Microsomal immobilized-enzyme-reactor for on-line production of glucuronides in a HPLC column. Chromatographia 37, 608–612. https://doi.org/10.1007/BF02274110.

Backman, J.T., Honkalammi, J., Neuvonen, M., Kurkinen, K.J., Tornio, A., Niemi, M., Neuvonen, P.J., 2009. CYP2C8 activity recovers within 96 hours after Gemfibrozil dosing: estimation of CYP2C8 half-life using Repaglinide as an in vivo probe. Drug Metab. Dispos. 37, 2359–2366. https://doi.org/10.1124/dmd.109.029728.

Boase, S., Miners, J.O., 2002. In vitro–in vivo correlations for drugs eliminated by glucuronidation: Investigations with the model substrate zidovudine. Br. J. Clin. Pharmacol. 54, 493–503. https://doi.org/10.1046/j.1365-2125.2002.01669.x.

EMA, 2012. Guideline on the investigation of drug interactions.

Engtrakul, J.J., Foti, R.S., Strelevitz, T.J., Fisher, M.B., 2005. Altered Azt (3′-Azido-3′-deoxythymidine) glucuronidation kinetics in liver microsomes as an explanation for underprediction of in vivo clearance: comparison to hepatocytes and effect of incubation environment. Drug Metab. Dispos. 33, 1621–1627. https://doi.org/10.1124/dmd.105.005058.

FDA, 2020. In vitro drug interaction studies — cytochrome P450 enzyme- and transporter-mediated drug interactions guidance for industry.

Fisher, M.B., Campanale, K., Ackermann, B.L., VandenBranden, M., Wrighton, S.A., 2000. In vitro glucuronidation using human liver microsomes and the pore-forming peptide alamethicin. Drug Metab. Dispos. 28, 560–566.

Hochman, Y., Zakim, D., Vessey, D.A., 1981. A kinetic mechanism for modulation of the activity of microsomal UDP-glucuronyltransferase by phospholipids. Effects of lysophosphatidylcholines. J. Biol. Chem. 256, 4783–4788.

Hochner-Celnikier, D., 1999. Pharmacokinetics of raloxifene and its clinical application. Eur. J. Obstet. Gynecol. Reprod. Biol. 85, 23–29. https://doi.org/10.1016/S0301-2115(98)00278-4.

Issa, N.T., Wathieu, H., Ojo, A., Byers, S.W., Dakshanamurthy, S., 2017. Drug metabolism in preclinical drug development: a survey of the discovery process, toxicology, and computational tools. Curr. Drug Metab. 18, 556–565. https://doi.org/10.2174/1389200218666170316093301.

Kazmi, S.R., Jun, R., Yu, M.-S., Jung, C., Na, D., 2019. In silico approaches and tools for the prediction of drug metabolism and fate: a review. Comput. Biol. Med. 106, 54–64. https://doi.org/10.1016/j.compbiomed.2019.01.008.

Kiiski, I.M.A., Pihlaja, T., Urvas, L., Witos, J., Wiedmer, S.K., Jokinen, V.P., Sikanen, T. M., 2019. Overcoming the pitfalls of cytochrome P450 immobilization through the Use of Fusogenic liposomes. Adv. Biosyst. 3, 1800245. https://doi.org/10.1002/adbi.201800245.

Kim, H.S., Wainer, I.W., 2005. The covalent immobilization of microsomal uridine diphospho-glucuronosyltransferase (UDPGT): initial synthesis and characterization of an UDPGT immobilized enzyme reactor for the on-line study of glucuronidation. J. Chromatogr. B 823, 158–166. https://doi.org/10.1016/j.jchromb.2005.06.030.

Klimas, R., Mikus, G., 2014. Morphine-6-glucuronide is responsible for the analgesic effect after morphine administration: a quantitative review of morphine, morphine-6-glucuronide, and morphine-3-glucuronide. Br. J. Anaesth. 113, 935–944. https://doi.org/10.1093/bja/aeu186.

Lee, J., Kim, S.H., Kim, Y.-C., Choi, I., Sung, J.H., 2013. Fabrication and characterization of microfluidic liver-on-a-chip using microsomal enzymes. Enzyme Microb. Technol. 53, 159–164. https://doi.org/10.1016/j.enzmictec.2013.02.015.

Liu, Y., Coughtrie, M.W.H., 2017. Revisiting the latency of uridine diphosphate-glucuronosyltransferases (UGTs)—how does the endoplasmic reticulum membrane influence their function? Pharmaceutics 9, 32. https://doi.org/10.3390/pharmaceutics9030032.

Manevski, N., Moreolo, P.S., Yli-Kauhaluoma, J., Finel, M., 2011. Bovine Serum Albumin Decreases Km Values of Human UDP-Glucuronosyltransferases 1A9 and 2B7 and Increases Vmax Values of UGT1A9. Drug Metab. Dispos. 39, 2117–2129. https://doi.org/10.1124/dmd.111.041418.

Munirathinam, R., Huskens, J., Verboom, W., 2015. Supported catalysis in continuous-flow microreactors. Adv. Synth. Catal. 357, 1093–1123. https://doi.org/10.1002/adsc.201401081.

Nicoli, R., Bartolini, M., Rudaz, S., Andrisano, V., Veuthey, J.-L., 2008. Development of immobilized enzyme reactors based on human recombinant cytochrome P450 enzymes for phase I drug metabolism studies. J. Chromatogr. A 1206, 2–10. https://doi.org/10.1016/j.chroma.2008.05.080.

Palacharla, R.C., Uthukam, V., Manoharan, A., Ponnamaneni, R.K., Padala, N.P., Boggavarapu, R.K., Bhyrapuneni, G., Ajjala, D.R., Nirogi, R., 2017. Inhibition of cytochrome P450 enzymes by saturated and unsaturated fatty acids in human liver microsomes, characterization of enzyme kinetics in the presence of bovine serum albumin (0.1 and 1.0% w/v) and in vitro – in vivo extrapolation of hepatic clearance. Eur. J. Pharm. Sci. 101, 80–89. https://doi.org/10.1016/j.ejps.2017.01.027.

Palaiokostas, M., Ding, W., Shahane, G., Orsi, M., 2018. Effects of lipid composition on membrane permeation. Soft Matter 14, 8496–8508. https://doi.org/10.1039/C8SM01262H.

Regan, S.L., Maggs, J.L., Hammond, T.G., Lambert, C., Williams, D.P., Park, B.K., 2010. Acyl glucuronides: the good, the bad and the ugly. Biopharm. Drug Dispos. 31, 367–395. https://doi.org/10.1002/bdd.720.

Rowland, A., Gaganis, P., Elliot, D.J., Mackenzie, P.I., Knights, K.M., Miners, J.O., 2007. Binding of inhibitory fatty acids is responsible for the enhancement of UDP-glucuronosyltransferase 2B7 activity by albumin: implications for in vitro-in vivo extrapolation. J. Pharmacol. Exp. Ther. 321, 137–147. https://doi.org/10.1124/jpet.106.118216.

Sakai-Kato, K., Kato, M., Toyo'oka, T., 2004. Screening of inhibitors of uridine diphosphate glucuronosyltransferase with a miniaturized on-line drug-metabolism system. J. Chromatogr. A 1051, 261–266. https://doi.org/10.1016/j.chroma.2004.06.058.

Schejbal, J., Řemínek, R., Zeman, L., Mádr, A., Glatz, Z., 2016. On-line coupling of immobilized cytochrome P450 microreactor and capillary electrophoresis: a promising tool for drug development. J. Chromatogr. A 1437, 234–240. https://doi.org/10.1016/j.chroma.2016.01.081.

Sheldon, R.A., 2007. Enzyme immobilization: the quest for optimum performance. Adv. Synth. Catal. 349, 1289–1307. https://doi.org/10.1002/adsc.200700082.

Sikanen, T., Zwinger, T., Tuomikoski, S., Franssila, S., Lehtiniemi, R., Fager, C.-M., Kotiaho, T., Pursula, A., 2008. Temperature modeling and measurement of an electrokinetic separation chip. Microfluid. Nanofluidics 5, 479–491. https://doi.org/10.1007/s10404-008-0260-1.

Smith, J.N., 1953. Studies in detoxication. 53. The glucuronic acid conjugation of hydroxyquinolines and hydroxypyridines in the rabbit. Biochem. J. 55, 156–160. https://doi.org/10.1042/bj0550156.

Soars, M.G., 2002. In vitro analysis of human drug glucuronidation and prediction of in vivo metabolic clearance. J. Pharmacol. Exp. Ther. 301, 382–390. https://doi.org/10.1124/jpet.301.1.382.

Soars, M.G., Burchell, B., Riley, R.J., 2002. In vitro analysis of human drug glucuronidation and prediction of in vivo metabolic clearance. J. Pharmacol. Exp. Ther. 301, 382–390. https://doi.org/10.1124/jpet.301.1.382.

Suryawanshi, P.L., Gumfekar, S.P., Bhanvase, B.A., Sonawane, S.H., Pimplapure, M.S., 2018. A review on microreactors: reactor fabrication, design, and cutting-edge applications. Chem. Eng. Sci. 189, 431–448. https://doi.org/10.1016/j.ces.2018.03.026.

Tornio, A., Filppula, A.M., Kailari, O., Neuvonen, M., Nyrönen, T.H., Tapaninen, T., Neuvonen, P.J., Niemi, M., Backman, J.T., 2014. Glucuronidation converts clopidogrel to a strong time-dependent inhibitor of CYP2C8: a phase II metabolite as a perpetrator of drug–drug interactions. Clin. Pharmacol. Ther. 96, 498–507. https://doi.org/10.1038/clpt.2014.141.

Tukey, R.H., Strassburg, C.P., 2000. Human UDP-glucuronosyltransferases: metabolism, expression, and disease. Annu. Rev. Pharmacol. Toxicol 40, 581–616. https://doi.org/10.1146/annurev.pharmtox.40.1.581.

Vessey, D.A., Zakim, D., 1971. Regulation of microsomal enzymes by phospholipids. II. Acitvation of hepatic uridine diphosphate-glucuronyltransferase. J. Biol. Chem. 246, 4649–4656.

Williams, J.A., Hyland, R., Jones, B.C., Smith, D.A., Hurst, S., Goosen, T.C., Peterkin, V., Koup, J.R., Ball, S.E., 2004. Drug-drug interactions for UDP-glucuronosyltransferase substrates: a pharmacokinetic explanation for typically observed low exposure (AUCi/AUC) ratios. Drug Metab. Dispos. 32, 1201–1208.